

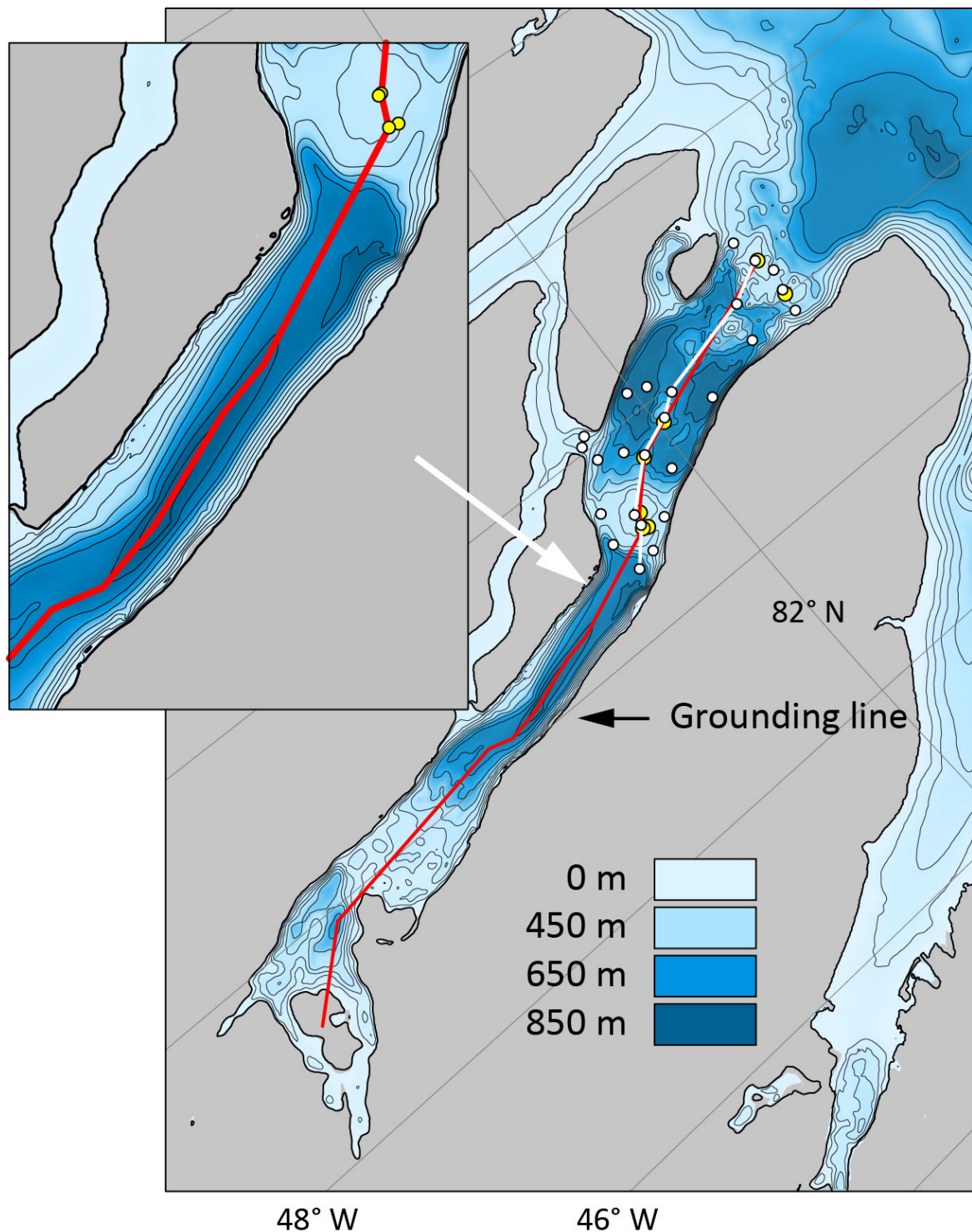
The Holocene dynamics of Ryder Glacier and ice tongue in north Greenland

Matt O'Regan et al.,

1. CTD and bathymetric profile (Fig. S1)

Detailed views of the location of the CTD (white) and bathymetric (red) profiles presented in the manuscript (Figs. 3 and 10). CTD stations are shown as white dots, and coring stations as yellow dots. The CTD profile intersects 11-GC on the outer sill instead of 10-GC, and does not cross the maximum sill depths on either the inner or outer fjord. The bathymetric profile follows the deepest channel beneath the ice tongue to avoid introducing artefacts that would otherwise appear to be steps in the seafloor morphology. Again, the profile does not pass through the maximum sill depth at the head of Sherard Osborn Fjord before reaching the restricted inner embayment.

Fig. S1:



2. Composite Depth Scales and depths of LU boundaries (Tables S1 and S2)

At coring stations 7, 8 and 9, piston, gravity and trigger weight cores were recovered. MSCL, Itrax XRF and CT-images were used to align these cores and construct composite depth scales. This involved stretching and squeezing of some intervals. At each site, we have kept the longer piston core depth scale undistorted. In 8-PC the gravity core recovered additional near surface material that was not preserved or recovered in 8-PC. Therefore, in the composite depth scale, the surface of 8-PC was shifted down but not distorted in any way. Here we provide the tie points used to generate the composite depth scales, which are critical for integrating measurements, such as ^{14}C dates, between cores from the same site (Table S1). Composite depths for the LU boundaries are given in Table S2.

Table S1: Tie points used to generate composite depth scales.

Core	Piston Core (PC)			Gravity Core (GC)			Trigger Weight Core (TWC)			
	Composite Depth (m)	Section	Interval (cm)	PC Depth (m)	Section	Interval (cm)	GC Depth (m)	Section	Interval (cm)	TWC Depth (m)
7	0	1	0	0						
7	0.08	1	8	0.08	1	0	0.00			
7	0.54	1	54	0.54	1	39	0.39	1	0	0.00
7	0.65	1	65	0.65	1	46	0.46	1	12	0.12
7	0.85	1	85	0.85	1	56	0.56	1	28	0.28
7	1.11	1	111	1.11	2	6	0.74	1	50	0.50
7	1.38	1	138	1.38	2	31	0.99	1	74	0.74
7	1.84	2	33	1.84	2	74	1.42			
7	2.06	2	55	2.06	2	94	1.62			
7	2.98	2	147	2.98	3	16	2.35			
7	3.22	3	22	3.22	3	38	2.57			
7	3.72	3	72	3.72	3	79	2.98			
7	4.20	3	120	4.20	3	120	3.39			
7	4.47	3	147	4.47	3	139	3.58			
7	4.62	4	11	4.62	4	3	3.73			
7	4.85	4	34	4.85	4	22	3.91			
7	5.06	4	54	5.06	4	36	4.06			
7	5.28	4	76	5.28	4	54	4.23			
7	5.65	4	113	5.65	4	81	4.50			
7	6.11	5	8	6.11	4	126	4.95			
7	8.31	6	78	8.31						
8	0.00				1	0	0.00			
8	0.38	1	0	0.00	1	38	0.38			
8	0.75	1	37	0.37	2	20	0.66			
8	1.02	1	64	0.64	2	40	0.86	1	0	0.00
8	1.41	1	103	1.03	2	71	1.17	1	30	0.30
8	1.80	1	142	1.42	2	103	1.49	1	62	0.62
8	2.09	2	20	1.71	2	133	1.79	1	92	0.92
8	2.83	2	94	2.45	3	47	2.45			

8	3.18	2	129	2.80	3	87	2.85				
8	4.00	3	62	3.62	3	143	3.41				
8	4.54	3	116	4.16	4	43	3.91				
8	4.93	4	6	4.55	4	61	4.10				
8	5.36	4	49	4.98	4	85	4.33				
8	5.57	4	70	5.19	4	104	4.52				
8	9.35	5	297	8.97							
9											
9	0.00	1	0	0.00							
9	0.18	1	18	0.18	1	0	0.00				
9	0.51	1	51	0.51	1	36	0.36				
9	0.65	1	65	0.65	1	46	0.46				
9	0.79	1	79	0.79	1	58	0.58				
9	0.94	1	94	0.94	1	71	0.71	1	0	0	
9	1.08	1	108	1.08	1	84	0.84	1	15	0.15	
9	1.30	1	130	1.30	1	110	1.10	1	36	0.36	
9	1.37	1	137	1.37	1	116	1.16	1	44	0.44	
9	1.41	1	141	1.41	1	120	1.20	1	48	0.48	
9	1.63	2	12	1.63	2	7	1.45	1	69	0.69	
9	1.84	2	33	1.84	2	28	1.66	1	86	0.86	
9	2.16	2	64	2.16	2	56	1.94				
9	2.29	2	77	2.29	2	70	2.08				
9	2.82	2	131	2.82	2	119	2.57				
9	3.20	3	19	3.20	3	5	2.94				
9	3.83	3	81	3.83	3	68	3.57				
9	3.94	3	92	3.94	3	83	3.72				
9	4.10	3	109	4.10	3	98	3.87				
9	4.53	4	0	4.53	3	139	4.28				
9	5.01	4	49	5.01	4	34	4.73				
9	5.13	4	61	5.13	4	41	4.80				
9	5.28	4	76	5.28	4	62	5.01				
9	5.55	4	103	5.55	4	91	5.30				
9	5.71	4	119	5.71	4	104	5.43				
9	5.90	4	138	5.90	4	116	5.55				
9	6.12	5	6	6.12	4	128	5.67				
9	6.42	5	36	6.42	4	146	5.85				

Table S2: Composite depths for the base of lithologic units in gravity and piston cores. Depths are in centimeters.

Core	LU1a	LU1b	LU2	LU3	LU4	LU5	LU6a	LU6b
10-GC	43	-	50	99	236	287	-	-
6-GC	43	-	109	136	246	493	-	-
7-PC	61		185	208	362	868	896	-
8-PC	103	315	401	455	634	712	762	935
9-PC	144	513	554	574	795	868	871.5	-

3. Detailed CT images (Figs. S2-S6)

Here we provide vertically uncompressed CT images from the cores discussed in the text and highlight the lithologic units. The CT images are 0.6 mm coronal slices with a pixel resolution of 500 x 500 microns.

Fig. S2:

Ryder19-10GC

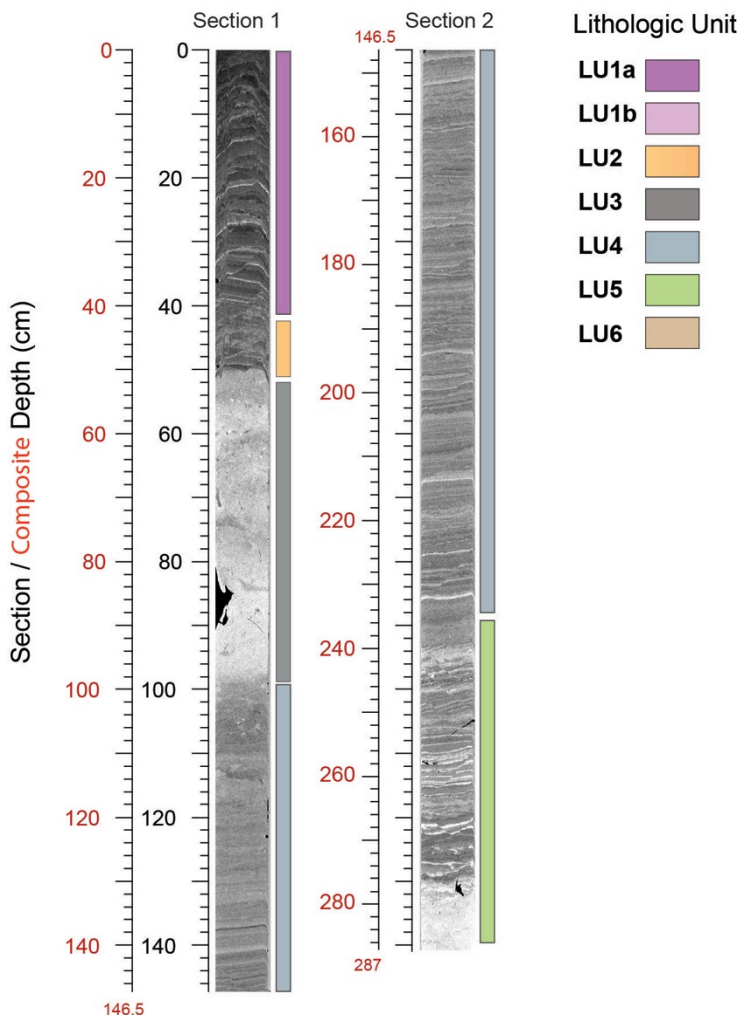


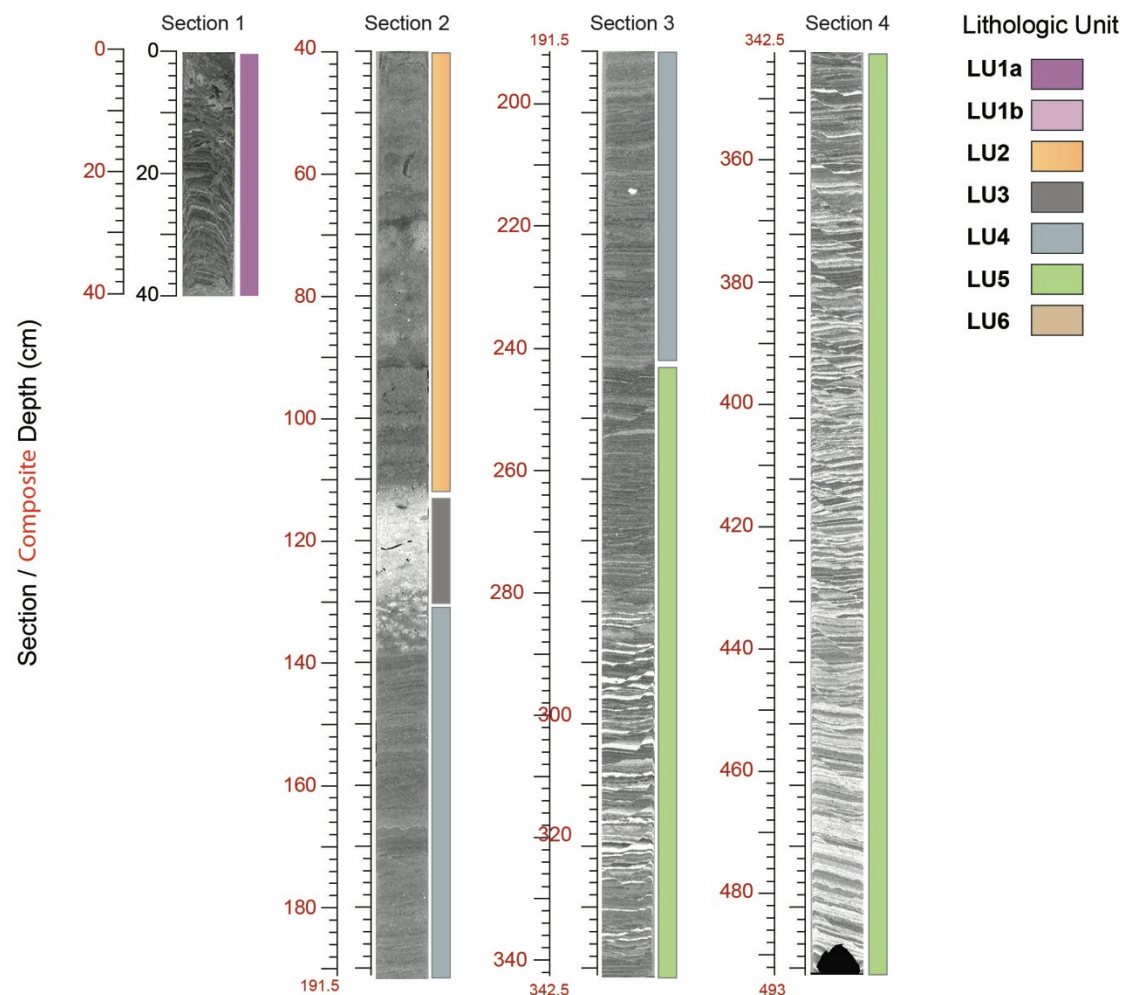
Fig. S3:**Ryder19-6GC**

Fig. S4:

Ryder19-7PC

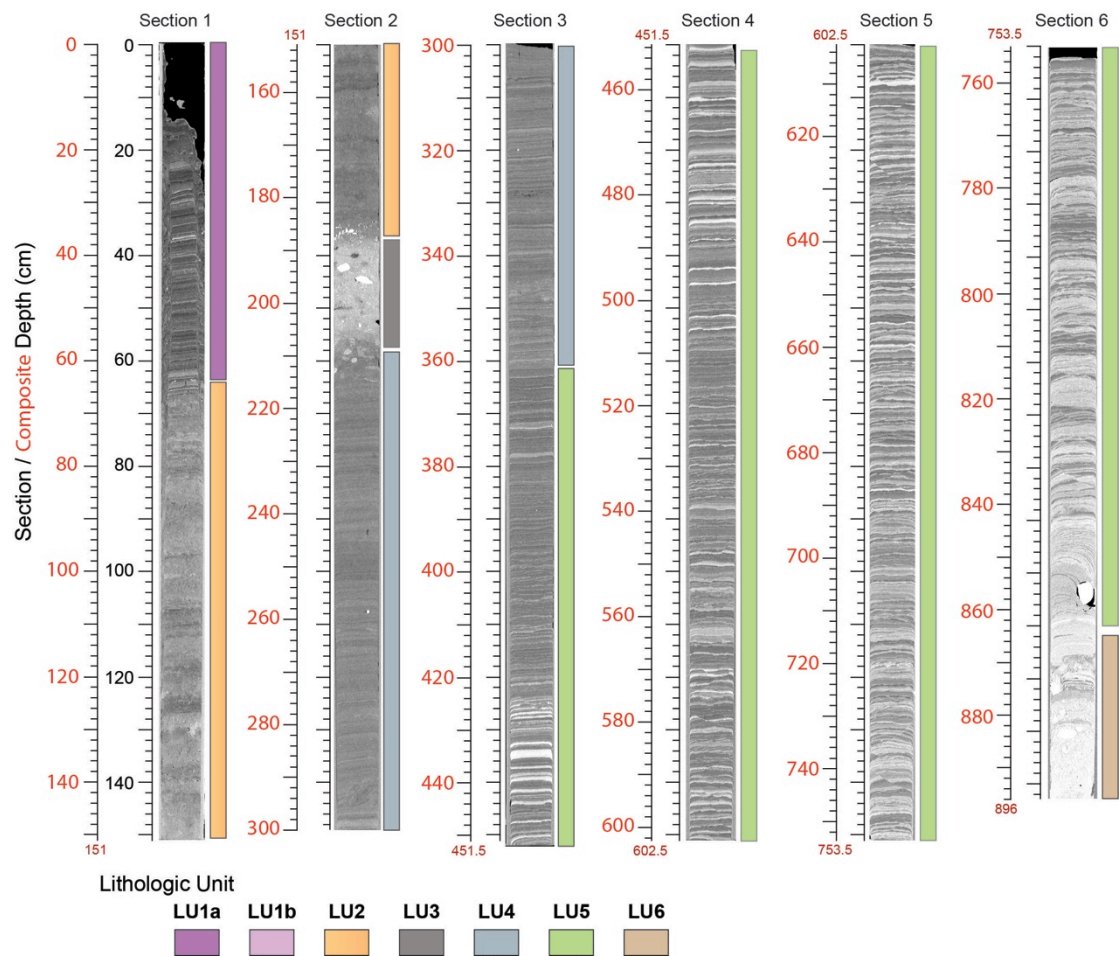


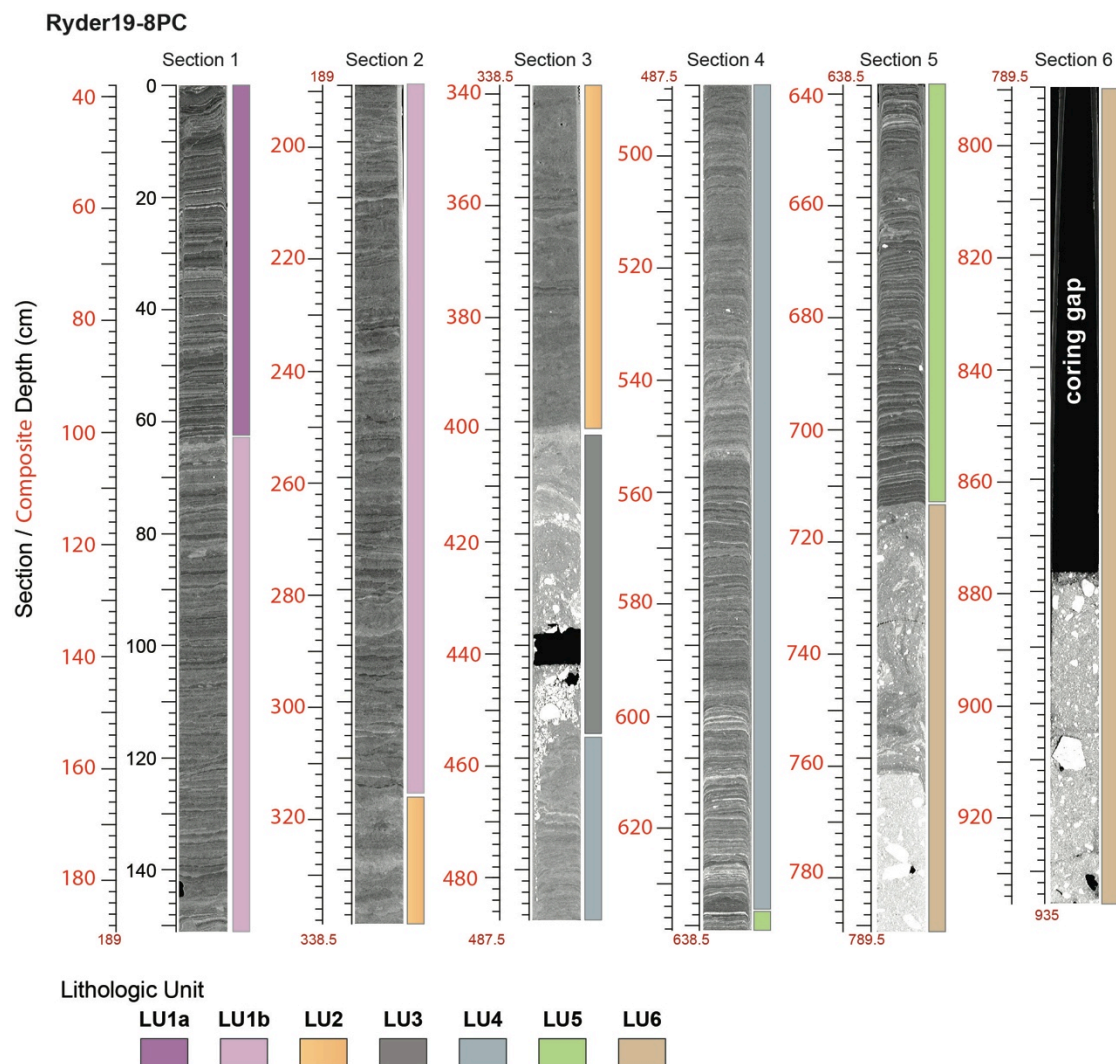
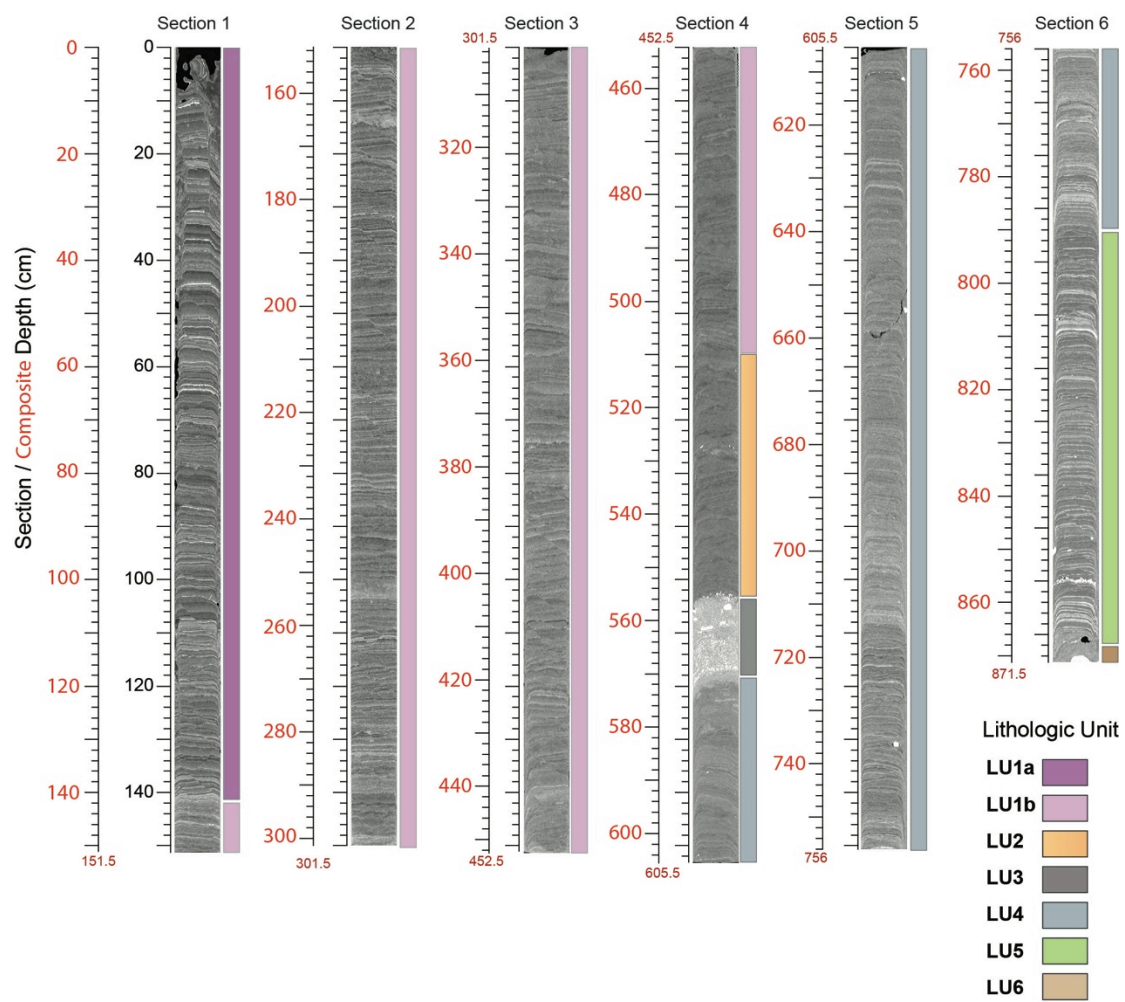
Fig. S5:

Fig. S6:
Ryder19-9PC



4. Adjustments to Bedmachine V3 (Fig. S7)

The digital elevation model (DEM) from Bedmachine V3 for Sherard Osborn Fjord was updated. The new model incorporates the multi-beam mapping data from Ryder 2019, which vastly improves the seafloor morphology in the outer fjord - in front (and immediately beneath) Ryders ice tongue. Considerable revisions also occur beneath the ice tongue in front of the grounding line. In order to map the bathymetry under the ice shelf between today's grounding line and the mapped inner sill, we interpolated the bed along 6 flowlines and used a minimum curvature interpolation to fill the gaps. The bathymetry under the ice shelf remains the least constrained region of BedMachine in this region. The revised DEM portrays a less constricted, broader, and more steeply sided trough. The yellow line marks the average modern ice limits with the ice tongue extending seaward of the grounding zone.

Fig. S7:

